Antarctic Science 17 (3), 418–426 (2005) © Antarctic Science Ltd Printed in the UK DOI: 10.1017/S0954102005002841

Costa Recta beach, Deception Island, West Antarctica: a retreated scarp of a submarine fault?

FERMÍN FERNÁNDEZ-IBÁÑEZ[1]*, RAUL PÉREZ-LÓPEZ[2], JOSÉ J. MARTÍNEZ-DÍAZ[3], CARLOS PAREDES[4], JORGE L. GINER-ROBLES[3], ALBERTO T. CASELLI[5] and JESÚS M. IBÁÑEZ[6]

[1]Dpto. de Geodinámica, F. de Ciencias, Campus Fuentenueva s/n, Universidad de Granada, 18002, Granada, Spain
[2]Dpto. de C.C. Ambientales y Rec. Naturales, Facultad de Farmacia, Universidad San Pablo-CEU, 28688 Boadilla del Monte, Madrid, Spain
[3] Dpto. de Geodinámica, F. C.C. Geológicas, Universidad Complutense de Madrid, 28040, Madrid, Spain
[4]Dpto. de Matemática Aplicada y Métodos Informáticos, E.T.S. Ingenieros de Minas, Universidad Politécnica de Madrid 28003, Madrid, Spain
[5]Dpto. Cs. Geológicas, Fac. Cs. Ex. y Nat., Universidad de Buenos Aires, Argentina, Ciudad Universitaria, Pab.2, 1428, Buenos Aires, Argentina
[6] Instituto Andaluz de Geofísica, Campus de Cartuja s/n, Universidad de Granada, 18071 Granada, Spain
**fferiba@ugr.es*

Abstract: Deception Island (South Shetlands, Antarctica) is one of the most active volcanoes in Antarctica, having erupted recently in 1967, 1969 and 1970, damaging scientific stations on the island. It is also seismically very active. The island has attracted the attention of many researchers as it constitutes an undisturbed natural laboratory to study seismo-volcanic events and how they affect landscape modelling and evolution. One of the most remarkable geological and geomorphological features on Deception Island is the linearity of its easternmost coastal landform, the origin of which remains unknown. Some answers, based on presence of strike-slip fault or on the ice cap and beach geomorphological dynamics, have been reported in the literature. Our new work provides several indications of the existence of a dip-slip submarine fault, parallel to the coast (NNW–SSE), which suggests a tectonic origin for this morphological feature. Uplifted marine terraces, incision of a fluvial network over the ice cap, normal faulting parallel to the coast in the north and south rock heads bounding the beach and sharp shelf-break with rather constant slope, constitute some of this evidence. Terrace uplift and fluvial channel incision decreasing southward from Macaroni Point, indicates possible tilt movement across this inferred fault plane.

Received 3 August 2004, accepted 29 March 2005

Key words: active tectonics, fault escarpment, straight coast, tectonic geomorphology, uplifted terraces

Introduction and geological setting

The Deception Volcanic Complex (Smellie *et al.* 2002) on Deception Island, South Shetland Islands, Antarctica (Fig. 1a & b), forms the youngest island of the Bransfield Basin (< 780 kyr; Valencio *et al*. 1979, Smellie 2002, Baraldo *et al.* 2003). The island was constructed as a polygenetic volcanic edifice emplaced during crustal extension on a small ocean basin (Bransfield Strait) opened between the Antarctic Plate and the former Phoenix Plate (Lawver *et al.* 1995, González-Casado *et al.* 2000). Bransfield Strait is interpreted as an atypical back-arc basin from earthquake focal mechanisms and fault analysis (González-Casado *et al.* 2000). The regional strain analysis suggests a NE–SW orientation of σ_{Hmax} (González-Casado *et al.* 2000).

The volcanic structure and the morphology of the island are controlled in several areas by submarine faults inferred from the gross geology, bathymetric and seismic profiles (Smellie 1989, Lawver *et al.* 1996, Grácia *et al*. 1997). Microfracture field analysis, carried out in faults sets measured from outcrops in Deception Island by several authors (Rey *et al.* 1995, González-Casado *et al.* 1999), show that the main structures inside the island have a mean NE–SW strike and a subordinate NW–SE strike.

Volcanic deposits are divided in two main groups according to the volcano-tectonic dynamic evolution of the island (Fig. 1c). Both groups were defined in relation to a single episode of caldera collapse (Smellie 2001, 2002):

1) *Precaldera deposits* (Port Foster Group): formed mainly by pillow lava deposits (currently below sea level), products of explosive hydrovolcanic eruptions and pyroclastic flow deposits from large-volume caldera-forming eruption (Smellie 2001, 2002).
2) *Post-caldera deposits* (Mount Pond Group): Pyroclastic and effusive eruption deposits, with several cinder cones and widespread tuff cones with numerous volcanic centres.

Martí & Baraldo (1990) suggested a passive collapse of the caldera along orthogonal faults as the origin of the inner great bay, Port Foster. The influence of the regional major faults was postulated by Smellie (1989), Rey *et al.* (1995)

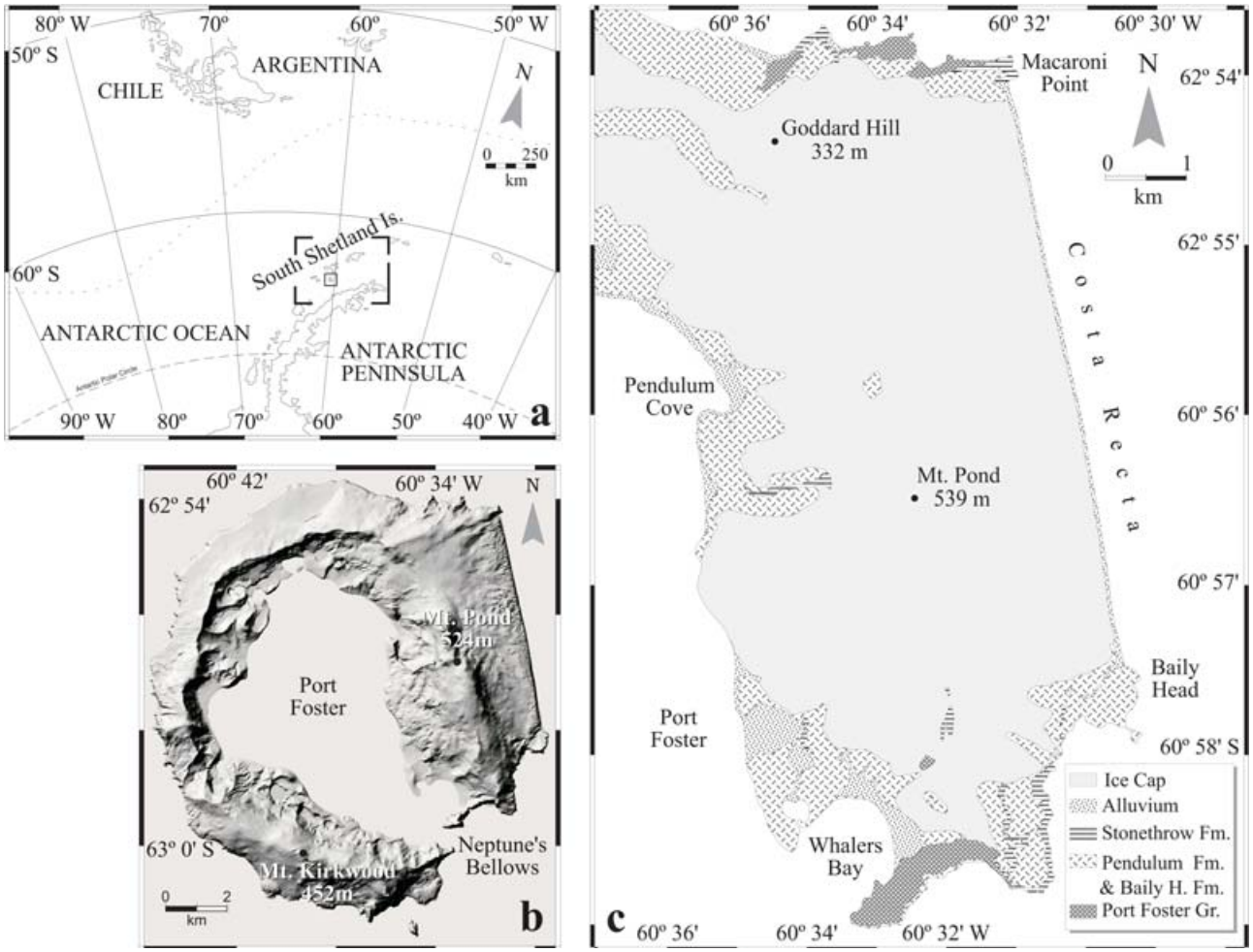

Fig. 1. Geographic localization and simplified geology of Deception Island. **a.** General map of the Antarctic Peninsula. **b.** Deception Island shaded relief map. **c.** Schematic geological map of the easternmost Deception Island (modified from Smellie *et al.* 2002).

and Martí *et al.* (1996). Smellie (2002) suggested a volcano-tectonic evolution and collapse of the caldera. At present time, caldera resurgence has been suggested by Cooper *et al.* (1998) and Smellie (2002). This hypothesis was supported by increased seismic activity during early 1992 (Ortiz *et al.* 1992) although there was no eruption. Three possible mechanisms may have triggered the last period of intense tectonic seismicity (1998–99).

1) a tectonic seismic swarm driven by regional stress field,

2) movement of magma inside the chamber, and

3) stress released by the uplift of the source area by magma injection at depth (Ibañez *et al.* 2000, 2003).

Two classical hypotheses have been proposed to explain Costa Recta origin and dynamics. The most widely accepted theory, which invokes tectonic control, explains the Costa Recta as a dextral strike-slip fault scarp (Rey *et al.* 1996). Later, Smellie (2002) explained the straight morphology as a reflection of tectonic constraints of the region, which are responsible for the dynamic evolution of the island. There is another hypothesis, proposed by López-Martínez & Serrano (2002), which points out the relevance of the interaction between the glacier and the beach dynamic. These authors conclude that the balance between glacier contribution and marine erosion is the origin of this rectilinearity.

It is possible to interpret a morpholineament oriented NNW–SSE for easternmost Deception Island, limited by two prominent volcanic headlands, Macaroni Point and Baily Head (Fig. 1c). However, until now there are no reported data or tectonic evidence that suggests the likeliest origin of this geomorphological feature. The aim of this paper is to present the results of some of the first reported geological field work along the Costa Recta beach with tectonosedimentary, geomorphological and structural observations.

Field work and site overview

Several stratigraphic and geological descriptions of Deception Island were carried out during the late 1990s and

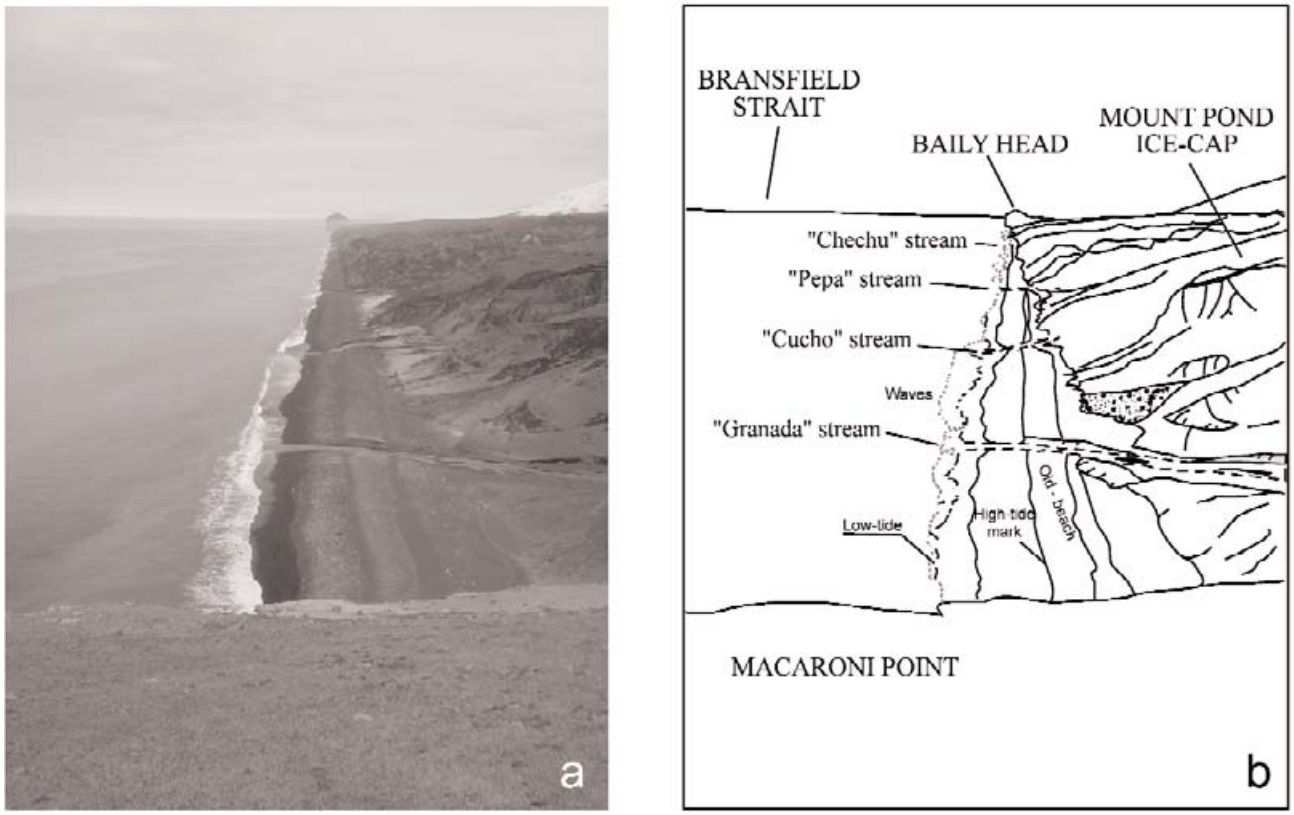

Fig. 2. Costa Recta overview. **a.** Photograph, and **b.** interpretation of the Costa Recta beach. The ice cliff is the frontal part of an ice cap coloured in grey by volcanic ashes. Four principal stream-cut channels are indicated in **b**.

early 21st century (Martí & Baraldo 1990, Birkenmajer 1992, 1995, Baraldo & Rinaldi 2000, Smellie 2002). However, among the available bibliography, no publications focused on Costa Recta, perhaps due to the lack of reported field data along the coast. The main relevance of this field trip along the Costa Recta was to reveal any geological evidence that supports one of the hypotheses previously proposed or to suggest a new one.

Costa Recta is a beach oriented NNE–SSW along 7.3 km of the island perimeter (almost 20% of the full perimeter of the island). An ice cliff a few tens of metres high extends along the Costa Recta being crossed by four main channels (Fig. 2), from Macaroni Point to Baily Head: "Granada", "Cucho", "Pepa" and "Chechu" streams (unofficial names).

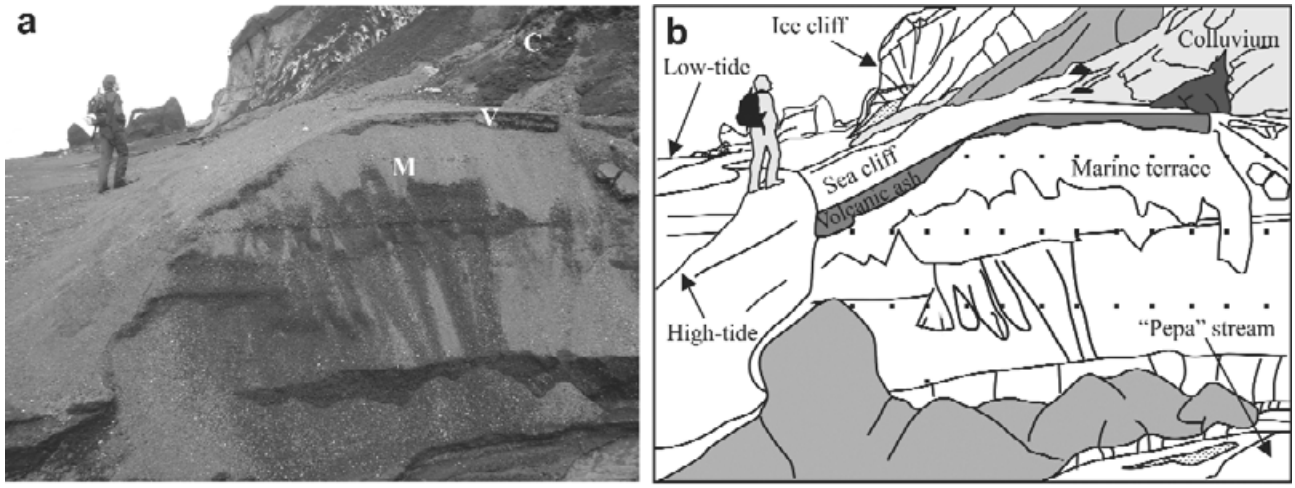

Fig. 3. Costa Recta terraces detail. **a.** Detailed photograph of one of the terraces, eroded by the incision of "Pepa" stream. **b.** Geological interpretation. G = Glacier, C = Colluvial deposits, V = Volcanic ash, M = Marine terraces.

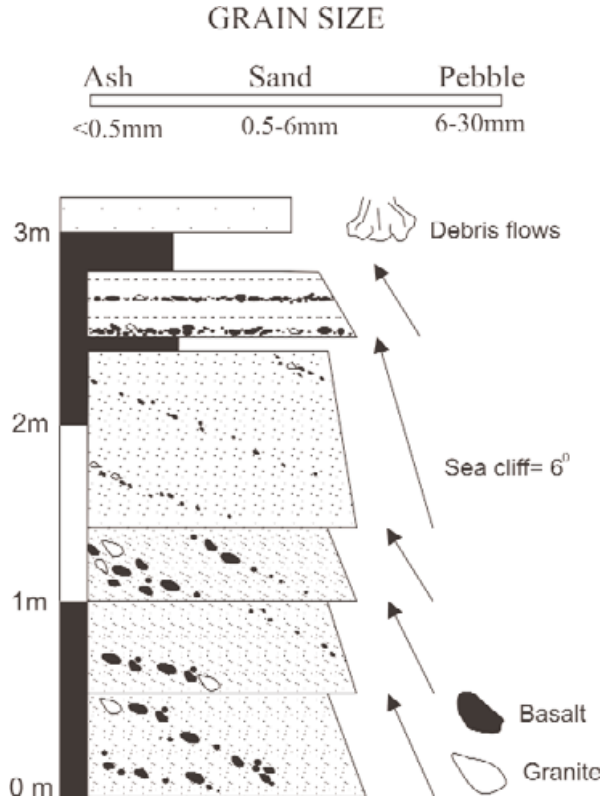

Fig. 4. Detailed stratigraphic log of a marine terrace recognized close to "Chechu" stream. Debris flows deposits cover the terraces. Arrows indicate strata decreasing sets. Black layer correspond to volcanic ash.

These streams provide alluvial material to the beach, which is removed by waves and tidal currents. The ice cliff corresponds to the leading edge of a glacier (glacier front) that we interpret as a relict (no current movement) glacier. One of the most remarkable features is the segmented character of the Costa Recta direction. Using GPS positioning, the orientation of the coast changes at the "Chechu" stream outfall point. The two coastal segments are oriented: N168ºE, 4.3 km long to the north and N172ºE, 2.9 km long to the south.

The Costa Recta beach shows several morphotectonic features of interest. It presents a well developed wave-cut platform of well sorted grains (ranging in size between 0.5–2 cm) and with a wide shoreline angle. Marine tides, reaching 1.8 m high (IHM 2004), show a sharp high-tide and low-tide peaks and two fluctuating intervening intermediate peaks. During low-tide period the beach is a wide flat surface, the wave-cut platform (Keller & Pinter 2002), whereas during high-tide there is a narrow surf-zone close to the shoreline (Fig. 2). Wave periods measured in this field trip were 6–12 sec long with waves from 50 to 70 cm high.

Pyroclastic grains of basaltic eroded volcanic rocks, transported by major streams described above, are dominant in beach deposits. Nevertheless some metamorphic and granite pebbles, possibly from Livingston Island, 70 km north of Deception Island, were collected. The smaller grain size ranges from 100 to 200 μm and appears only close to stream outlets. This indicates a hydrodynamic regime of the beach where fine grain deposits are removed while coarse grain deposits remain. Rounded and well-selected grain size points out to a high wave-energy coast. This erosional behaviour is evidenced by the intensely eroded recent alluvial fans observed along the coast.

Tectonic evidences

During this field visit several tectonic features were identified. These evidences address to a recent tectonic control of the Costa Recta landform.

Uplifted marine terraces

Few raised marine terraces were identified in the inner part of the beach, reaching maximum heights of 8 m above the present higher tidal level, near Macaroni Point, and decreasing southward to 3 m high. Well sorted coarse grain volcanic sands, with a resting angle close to 1º, are the dominant component of these terraces (Fig. 3). Macrofossil bearing deposits were not found in the marine terraces

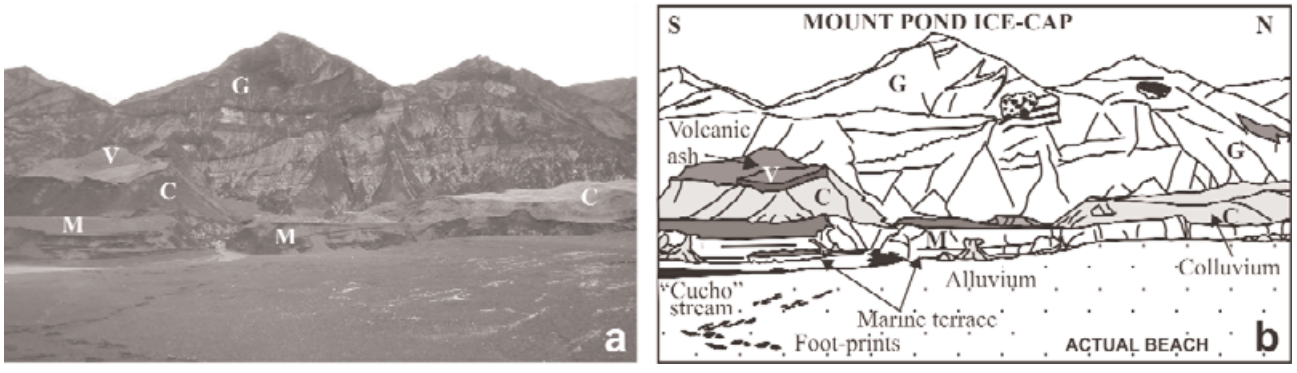

Fig. 5. General view of raised terraces in Costa Recta. **a.** Photograph, and **b.** geological interpretation. G = Glacier, C = Colluvial deposits, V = Volcanic ash, M = Marine terraces.

because of the poor biotopes developed in the inter-tidal zone. Under the erosive and high energy conditions of the beach, particles less than 2 mm are removed. The recent age of the island support this low level biological development.

Figure 4 shows a detailed stratigraphic record of a marine terrace close to "Chechu" stream (see also Fig. 3). The sequence is mainly composed of well-sorted coarse basaltic sands. Thin interlayered volcanic ash deposits are ubiquitous in the marine terraces, as well as some granitic and metamorphic clasts. Marine terraces are mostly covered by debris flows deposits.

Geomorphological observations show a modern seaward dipping slope of 33º and a horizontal older wave cut platform. The terraces have become partially covered by colluvial deposits from an older steep beach face and by wash from farther upslope. Some terraces are strongly eroded by the incision of streams draining the ice cap across the terrace surface. Most terraces are covered by a thin volcanic ash layer from recent eruptions (Fig. 5).

Incision of the drainage network

The drainage network on the ice cap has developed a characteristic pattern toward the north end of the coast where the streams shows a high rate of incision. Relief is higher in the southern part; however, the incision rate is higher in the northern part and decreases southwards (Fig. 6). This supports a tilting mechanism with a higher rate in the northern sector of Costa Recta. A change in local base level of erosion drives the evolution of the landscape and appears to be a mechanism by which the fluvial

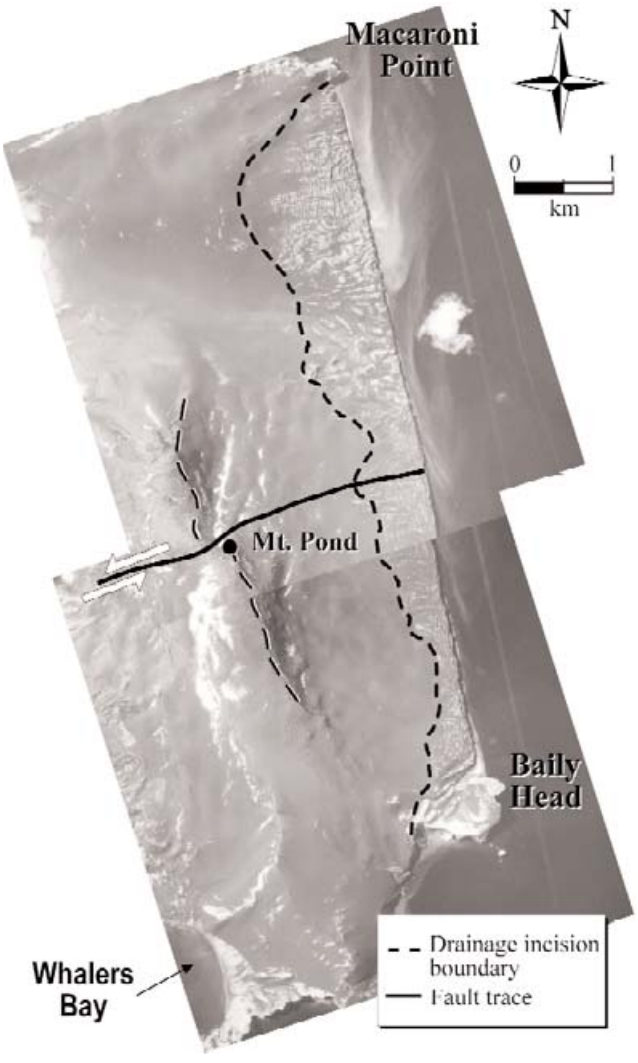

Fig. 6. Aerial photograph of Costa Recta showing incision pattern developed by drainage network over the glacier and major deformations induced by Mount Pond sinistral strike-slip fault.

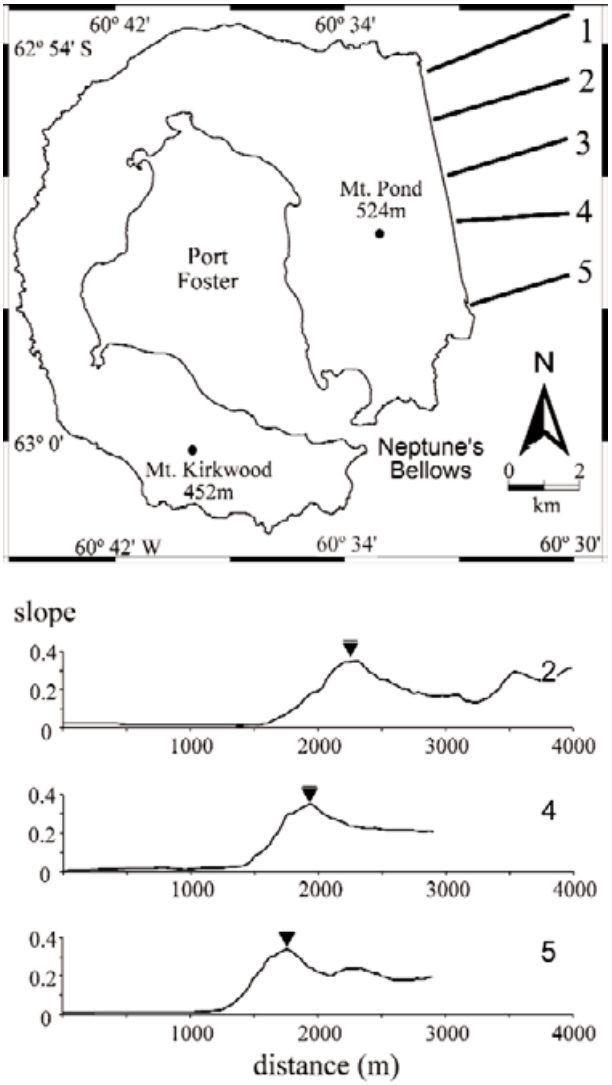

Fig. 7. Location of the set of bathymetric profiles calculated offshore Costa Recta beach. Slope profiles orthogonal to Costa Recta are shown below. Black triangles indicate the maximum slope rupture. A narrow zone with a sharp slope was recognized 1 km offshore. See text for details.

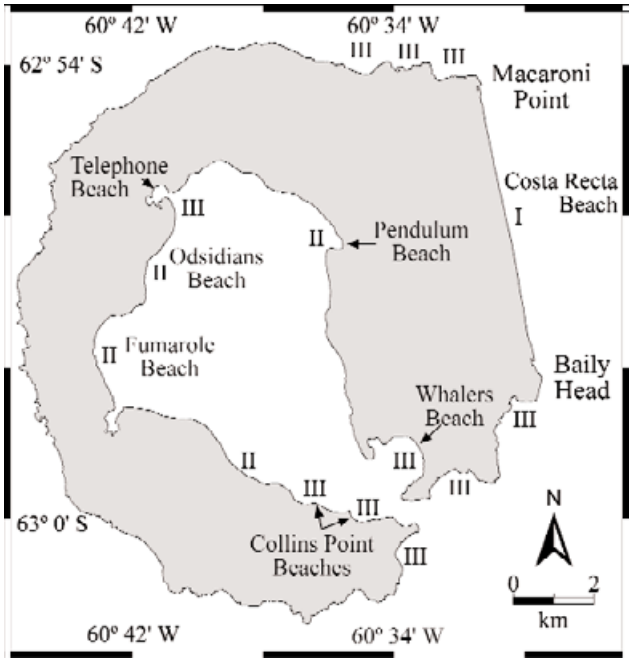

Fig. 8. Different sort of beaches differentiated in Deception Island. Type I: straight beaches; Type II: log-spiral beaches; Type III: hyperbolic beaches.

network responds to tectonic activity.

Bathymetry

A bathymetric grid was created offshore Costa Recta from around 16 000 depth values collected from six hydrographic campaigns. These bathymetric expeditions were carried out by Servicio Hidrográfico Nacional of Argentina (1995–96, 1997–98 and 1999–2000 Antarctic Summer Campaign), Spain (B.I.O. Hespérides, 1999 Port Foster Campaign) and Great Britain (1948–49, 1988 Neptune's Bellows Campaign).

Depth data have been interpolated by Voronoy Triangulation. The first derivative has been calculated for this bathymetric grid and consequently slope analysis has been done to bracket areas of steep slope. Five slope profiles were generated perpendicular to Costa Recta (Fig. 7). These profiles show a gently sloping shelf that runs offshore Costa Recta more than 1 km and ends in a sharp shelf-break showing an increasing slope with maximum value of 0.35 that remains constant for a few tens of metres. This constant attitude in slope reveals the presence of a narrow zone having a sharp slope dipping eastward. The entire set of bathymetric profiles shows how the slope decreases southwards.

Logarithmic spiral shorelines

Looking around Deception Island three sorts of beaches can be differentiated (Fig. 8), hyperbolic beaches (e.g. Whalers beach), logarithmic spiral beaches (e.g. Fumarole beach) and straight beaches (e.g. Costa Recta beach). Both hyperbolic and logarithmic planforms represent equilibrium morphologies for beaches bounded by one or two headlands, respectively. Logarithmic spiral (log-spiral) beaches (Krumbein 1944, Silvester 1960) appear along the external perimeter of the island and in the inner bay (Port Foster) and result from a combination of diffraction and refraction dynamic of marine waves. A log-spiral shoreline is the natural end result when erosive processes affect beaches located between headlands (LeBlond 1979).

Costa Recta beach, bounded by two headlands but, being straight, is an isolated case for the entire island. Moreno & Krauss (1999) pointed out that sharp variations of bathymetry or topography related to underlying geological structure may cause deviations from a log-spiral morphology.

Fault data

A set of 54 strike and dip direction fault data were collected near Costa Recta (mostly at Baily Head and Maccaroni Point). Fault analysis show three main sets of fault orientations: N15E, that runs sub-parallel to the Bransfield Basin axis (González-Casado *et al.* 1999); N155E, that is sub-parallel to the Costa Recta beach; and N80E parallel to the Mount Pond fault orientation (stereographic and rose plot in Fig. 8). In every case, faults show steep dips (mean dip: 70º) with apparent normal (occasionally reverse) sense of displacement and are arranged in conjugate sets. Some of these faults control the development of recent morpho-lineaments such as the Mount Pond fault or those located to the north of Goddard Hill (Fig. 6). The absence of any kinematically generated striae, because of the nature of the volcanic deposits, makes it difficult to identify the sense of displacement associated with most of these structures. However, observations outlined here, suggest that they would have horizontal fault-displacement, placing constraints on recent tectonic processes.

As shown above, the Costa Recta beach can be divided into two segments. The "Chechu" stream marks the point where the coast changes its orientation. This change coincides with the position of a major inferred sinistral strike-slip fault, the Mount Pond fault (Rey *et al.* 1995). This fault sinistrally displaces the major morphostructure of the Mount Pond range and also produces surface and internal evidence of ductile deformation in the ice cap (Fig. 6). This evidence is also seen in the digital elevation model and in the field work close to the cliff at the "Chechu" stream outlet.

Discussion

The existence of a set of N155E normal faults, mainly sampled in Baily Head and Macaroni Point, with directions

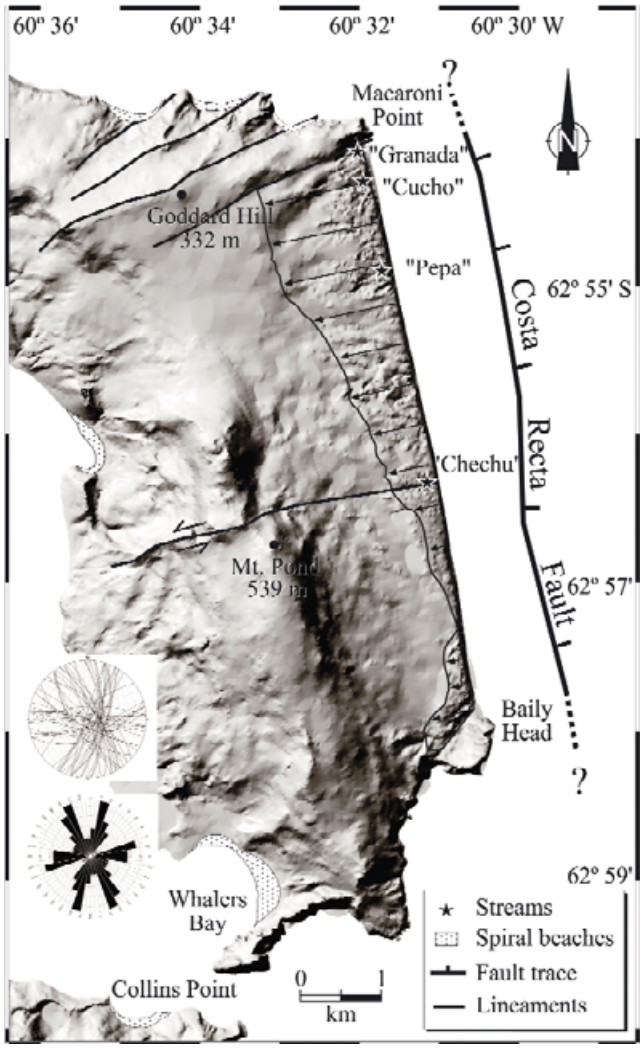

Fig. 9. Schematic tectonic map and digital elevation model of the Costa Recta beach showing interpreted major tectonic features. Inferred Costa Recta beach trace fault, based on bathymetry data, is also shown. Black arrows point to drainage incision boundary. Stereoplots represent main orientations of fault data collected in Macaroni Point and Baily Head outcrops. Equal angle lower-hemisphere projection.

very close to the general alignment of the coast, supports the idea of a major tectonic feature that determines the morphology of the Costa Recta. There are no focal mechanisms for locally recorded earthquakes and where hypocenters are available, they present large uncertainties that result from both the sparse networks and uncertainties in the velocity structure (Saccorotti *et al.* 2001). Therefore it is rather difficult to unravel the link between high-frequency earthquakes and some of these structures.

Marine terraces localized in the inner part of the beach reveal a local and constant tectonic uplift in the easternmost part of Deception Island. Moreover, there is an incipient incision of the drainage network in the ice cap, that has progressed northward, resulting in a well developed

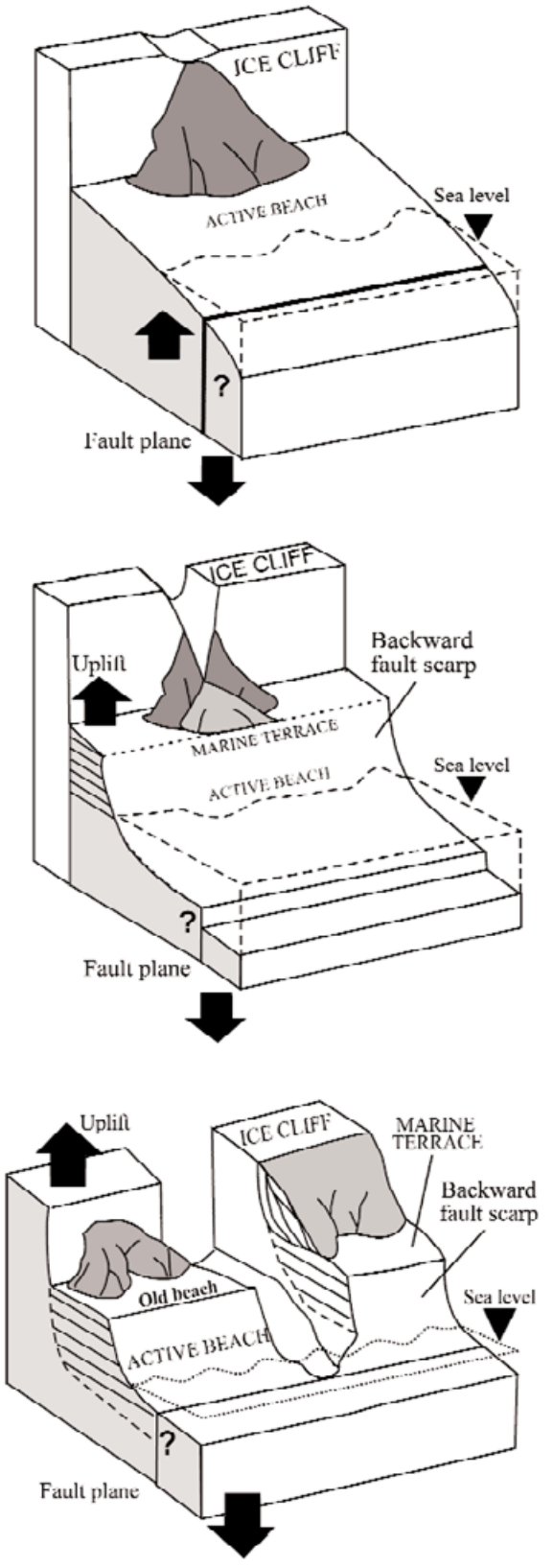

Fig. 10. Proposed evolution model. **a.** Beach with an ice cliff. **b.** Slip movement of submarine fault that raises the hanging wall block. Fault scarp retreats and fluvial network goes an incipient incision. **c.** Incision of fluvial network affects marine terraces.

incision pattern. This incision rate is higher in the block located to the north of Mount Pond fault.

According to the rates of incision of the drainage network we suggest a normal fault model with a southward decreasing amount of slip from Macaroni Point to Baily Head. This model agrees with the decreasing height of the marine terraces and the depth of incision of the drainage network to Baily Head. Figure 9 shows major morpholineaments for easternmost Deception Island. A probable fault trace for Costa Recta Beach, with decreasing slip southwards, is also shown.

On the other hand, the geometry and position of the glacier and the absence of an accumulation zone (s.s.) support the idea that the ice has not suffered significant horizontal displacements. Moreover, it is difficult to understand a coastline with a straight geometry more than 7 km long, along the front of an active glacier with irregular bed topography. Therefore, we interpret it as a relict glacier with no current motion.

Bathymetric profiles disclose a submarine scarp having a sharp slope with constant NNW–SSE attitude that runs sub-parallel to the Costa Recta. The existence of such scarp is compatible with our hypothesis of a submarine fault with the slip-down block offshore (Fig. 9). Moreover, decrease of slope toward the south agrees with the idea of fault tilt decreasing to the south of Deception Island.

Additional support for our model comes from the planform of the beach. Log-spiral shape of shorelines is the most common evolution of erosive beaches located between two headlands for coast with predominant wave direction. Well developed beaches show log-spiral planform (LeBlond 1979, Finkelstein 1982), this is the case of all those beaches localized in the inner part of the island and the few ones of the outer sides (e.g. Pendulum Cove beach, Whalers beach and Collins beach among others. See Fig. 8). The Costa Recta beach is located between Macaroni Point and Baily Head, with a predominant wave direction from north-east to south-west; nevertheless, it does not show log-spiral geometry and it may indicate that it is younger than the rest of the beaches of Deception Island. Hence, the linearity of Costa Recta points to the presence of an underlying geological structure that highly constrains its planform (Moreno & Krauss 1999).

Conclusions

The geomorphic and tectonic evidences described above (namely, marine terraces in Costa Recta, fluvial network incision on the relict glacier of Mount Pond, beach shape of Costa Recta, subordinate faults measured in Baily Head and Macaroni Point running sub-parallel to Costa Recta and bathymetric profiles showing a submarine scarp) point to the existence of a submarine fault scarp. Furthermore, the gradient incision of the fluvial network and the slope variation to the submarine scarp, both decrease to the south, suggest tilt movement on the fault.

Following these observations we suggest that the straight character of Costa Recta is the geomorphological expression of a retreated scarp produced by a submarine fault orientated NNW–SSE. Slip movement of a submarine fault raises the hanging wall block. Continued erosion degrades the scarp away from the fault itself to leave a fault-line scarp; fluvial networks creates incipient incision over the retreated fault scarp, also affecting marine terraces (Fig. 10). Such stream behaviour also suggests a system of blocks bounded by faults as a result of the interference of some major structures, Mount Pond system (N80E) and Costa Recta system (N160E). Alignment of 1967–70 volcanic centres (Valenzuela *et al.* 1968, Baker & McReath 1971) invokes that both systems may still be active under the current tectonic regime.

Recent tectonics in Deception Island constrains its current configuration. Despite the wealth of evidence presented in this paper, model must be constrained with further geophysical data in order to define the eastern margin of Deception Island and establish the links between this structure and active tectonic processes in the island.

Acknowledgements

We thank the Spanish Ministry for Science and Technology which provided the financial support for the projects VISHNU (REN2002-00578/ANT) and TOMODEC (REN2001-3833/ANT), and Secretaría de Ciencia y Tecnología Argentina and Dirección Nacional del Antártico (PICT-O 07-11557) which provided the financial support of the project and the use of Antarctic Argentine base "Decepción". We also thank Dr J.L. Smellie, Dr Asrarur R. Talukder and David Gallego for their helpful criticisms, comments and assistance with English grammar. We appreciate very much the Spanish and Argentinean Army for providing the use of both "Gabriel de Castilla" and "Decepción" Antarctic bases.

References

Baraldo, A. & Rinaldi, C.A. 2000. Stratigraphy and structure of Deception Island - South Shetland Islands, Antarctica. *Journal of South American Earth Sciences*, **13**, 785–796.

Baraldo, A., Rapalini, A.E., Böhnel, H. & Mena, M. 2003. Paleomagnetic study of Deception Island, South Shetland Islands, Antarctica. *Geophysical Journal International*, **153**, 1–11.

Barker, P.E. & Mcreath, I. 1971. 1970 volcanic eruption at Deception Island. *Nature*, **231**, 5–9.

Birkenmajer, K. 1992. Volcanic succession at Deception Island, West Antarctica: a revised lithostratigraphic standard. *Studia Geologica Polonica*, **101**, 131–143.

Birkenmajer, K. 1995. Volcano-structural evolution of the Deception Island volcano, West Antarctica. *Terra Antartica*, **2**, 33–40.

Cooper, A.P.R., Smellie, J.L. & Maylin, J. 1998. Evidence for shallowing from bathymetric records of Deception Island. *Antarctic Science*, **10**, 455–461.

FINKELSTEIN, K. 1982. Morphological variations and sediment transport in crenulate-bay beaches, Kodiac Island, Alaska. *Marine Geology*, **47**, 261–281.

GONZÁLEZ-CASADO, J.M., LÓPEZ-MARTÍNEZ, J., GINER, J., DURÁN, J.J. & GUMIEL, P. 1999. Análisis de la microfracturación en la Isla Decepción, Antartida Occidental. *Geogaceta*, **26**, 27–30.

GONZÁLEZ-CASADO, J.M., GINER-ROBLES, J.L. & LÓPEZ-MARTÍNEZ, J. 2000. Bransfield Basin, Antarctic Peninsula: not a normal backarc basin. *Geology*, **28**, 1043–1046.

GRÀCIA, E., CANALS, M., FARRÁN, M., SORRIBAS, J. & PALLÀS, R. 1997. Central and Eastern Bransfield Basins (Antarctica) from high-resolution swath-bathymetry data. *Antarctic Science*, **9**, 168–180.

IHM. 2004. *Anuario de mareas.* Vigo, Spain: Instituto Hidrográfico de la Marina.

IBÁÑEZ, J.M., DEL PEZZO, E., ALMENDROS, J., LA ROCCA, M., ALGUACIL, G., ORTIZ, R. & GARCÍA, A. 2000. Seismovolcanic signal at Deception Island volcano, Antarctica: wave field analysis and source modelling. *Journal of Geophysical Research*, **105**, 13905–13931.

IBÁÑEZ, J.M., ALMENDROS, J., CARMONA, E., MARTINEZ-AREVALO, C. & ABRIL, M. 2003. The recent seismo-volcanic activity at Deception Island volcano. *Deep Research II*, **50**, 1611–1629.

KELLER, E.A. & PINTER, N. 2002. *Active Tectonics*. Englewood Cliffs, NJ: Prentice Hall, 362 pp.

KRUMBEIN, W.C. 1944. Shore processes and beach characteristics. Washington, DC: US Army Corp of Engineers. *Beach Erosion Board Technical Memo*, **3**.

LAWVER, L.A., KELLER, R.A., FISK, M.R. & STRELIN, J.A. 1995. Bransfield Strait, Antarctic Peninsula: active extension behind a dead arc. *In* TAYLOR, B., *ed. Backarc basins: tectonics and magmatism.* New York: Plenum Press, 315–342.

LAWVER, L.A., SLOAN, B.J., BARKER, D.H.N., GHIDELA, M., VON HERZEN, R.P., KELLER, R.A., KLINKHAMMER, G.P. & CHIN, C.S. 1996. Distributed, active extension in Bransfield Basin, Antarctic Peninsula: evidence from multibeam bathymetry. *GSA Today*, **6**, 1–6 & 16–17.

LEBLOND, P.H. 1979. An explanation of the logarithmic spiral plan view of headland-by beaches. *Journal of Sedimentary Petrology*, **49**, 1093–1100.

LÓPEZ-MARTÍNEZ, J. & SERRANO, E. 2002. Geomorphology, supplementary text. *In* SMELLIE, J.L., LÓPEZ-MARTÍNEZ, J. *et al*., *eds. Geology and geomorphology of Deception Island.* Sheets 6-A and 6-B, 1:25000. *BAS GEOMAP Series.* Cambridge: British Antarctic Survey, 31–39.

MARTÍ, J. & BARALDO, A. 1990. Pre-caldera pyroclastic deposits of Deception Island (South Shetland Islands). *Antarctic Science*, **2**, 345–352.

MARTÍ, J., VILA, J. & REY, J. 1996. Deception Island (Bransfield Strait, Antarctica): an example of a volcanic caldera developed by extensional tectonic. *In* MCGUIRE, W.C., JONES, A.P. & NEUBERG, J., *eds. Volcano instabilities on the Earth and other planets. Geological Society of London Special Publications,* No. 10, 253–265.

MORENO, L.J. & KRAUSS, N.C. 1999. Equilibrium shape of headland-bay beaches for engineering design. *Proceedings Coastal Sediments.* **ASCE**, 860-875.

ORTIZ RAMIS, R., GARCÍA, A. & RISSO, C. 1992. *Seismic and volcanic activity in the South Shetlands Islands and the Antarctic Peninsula environment.* Madrid: Museo Nacional de Ciencias Naturales (CSIC). [*Unpublished report*]

REY, J., SOMOZA, L. & MARTÍNEZ-FRÍAS, J. 1995. Tectonic volcanic and hydrothermal event sequence on Deception Island (Antarctica). *Geo-Marine Letters*, **15**, 1–8.

REY, J., SOMOZA, L. & MARTÍNEZ-FRÍAS, J. 1996. Evidencias tectónicas, volcánicas e hidrotermales en Isla Decepción, relacionadas con el marco geodinámico de la cuenca de Bransfield (Antártida). *Actas del V Simposio de estudios Antárticos.* Madrid: Comisión Interministerial de Ciencia y Tecnología, 209–222.

SACCOROTTI, G., ALMENDROS, J., CARMONA, E., IBAÑEZ, J., DEL PEZZO, E. 2001. Slowness anomalies from two dense arrays at Deception Island, Antarctica. *Bulletin of the Seismological Society of America*, **91**, 557–571.

SILVESTER, R. 1960. Stabilization of sedimentary coastlines. *Nature*, **188**, 467–469.

SMELLIE, J.L. 1989. Deception Island. *In* DALZIEL, I.W.D., *ed. Tectonics of the Scotia Arc, Antarctica. 28th International Geological Congress, Field Trip Guide Book.* Washington, DC: American Geophysical Union, T180, 146–152.

SMELLIE, J.L. 2001. Lithostratigraphy and volcanic evolution of Deception Island, South Shetland Islands. *Antarctic Science*, **13**, 188–209.

SMELLIE, J.L. 2002. Geology. *In* SMELLIE, J.L., LÓPEZ-MARTÍNEZ, J., *et al. eds. Geology and Geomorphology of Deception Island.* Sheets 6-A and 6-B, 1:25000. *BAS* GEOMAP series. Cambridge: British Antarctic Survey, 11–30.

SMELLIE, J.L., LÓPEZ-MARTÍNEZ, J., *et al.* 2002. *Geology and geomorphology of Deception Island. BAS GEOMAP SERIES* Sheets 6-A and 6-B, 1:25 000. Cambridge: British Antarctic Survey.

VALENCIO, D.A., MENDÍA, J.E. & VILAS, J.F. 1979. Paleomagnetism and K–Ar age of Mesozoic and Cenozoic igneous rocks from Antarctica. *Earth & Planetary Science Letters*, **45**, 61–68.

VALENZUELA, E., CHAVEZ, B.L. & MUNIZAGA, V.F. 1968. Informe preliminar sobre la erupción de Isla Decepción ocurrida en Diciembre de 1967. *Boletín del Instituto Antártico Chileno*, **3**, 5–16.